



July 2003

Determining the $\text{Ce}_2\text{O}_2\text{S-CeO}_x$ Phase Boundary for Conditions Relevant to Adsorption and Catalysis

Robert M. Ferrizz
University of Pennsylvania

Raymond J. Gorte
University of Pennsylvania, gorte@seas.upenn.edu

John M. Vohs
University of Pennsylvania, vohs@seas.upenn.edu

Follow this and additional works at: https://repository.upenn.edu/cbe_papers

Recommended Citation

Ferrizz, R. M., Gorte, R. J., & Vohs, J. M. (2003). Determining the $\text{Ce}_2\text{O}_2\text{S-CeO}_x$ Phase Boundary for Conditions Relevant to Adsorption and Catalysis. Retrieved from https://repository.upenn.edu/cbe_papers/41

Postprint version. Published in *Applied Catalysis B: Environmental*, Volume 43, Issue 3, 10 July 2003, pages 273-280.

Publisher URL: [http://dx.doi.org/10.1016/S0926-3373\(02\)00323-5](http://dx.doi.org/10.1016/S0926-3373(02)00323-5)

This paper is posted at ScholarlyCommons. https://repository.upenn.edu/cbe_papers/41
For more information, please contact repository@pobox.upenn.edu.

Determining the Ce₂O₂S-CeO_x Phase Boundary for Conditions Relevant to Adsorption and Catalysis

Abstract

The interaction of sulfur with ceria under highly reducing conditions was investigated. The phase boundary between CeO_{1.83} and Ce₂O₂S was determined for temperatures between 873 and 1073 K. This data was used to derive an empirical equation for ΔG_f° of Ce₂O₂S in this temperature range. This equation along with thermodynamic data for cerium oxides and sulfides obtained from the literature was used to predict Ce-O-S phase diagrams at 873 and 973 K. These phase diagrams provide insight into the mechanism of the deactivation of ceria-based catalysts by sulfur under reducing conditions.

Keywords

Ceria, Cerium oxysulfide, Sulfur, Adsorption

Comments

Postprint version. Published in *Applied Catalysis B: Environmental*, Volume 43, Issue 3, 10 July 2003, pages 273-280.

Publisher URL: [http://dx.doi.org/10.1016/S0926-3373\(02\)00323-5](http://dx.doi.org/10.1016/S0926-3373(02)00323-5)

**Determining the Ce₂O₂S-CeO_x Phase Boundary for Conditions
Relevant to Adsorption and Catalysis**

by

R.M. Ferrizz, R.J. Gorte, and J.M. Vohs

Department of Chemical and Biomolecular Engineering
University of Pennsylvania
Philadelphia, PA 19104

Abstract

The interaction of sulfur with ceria under highly reducing conditions was investigated. The phase boundary between CeO_{1.83} and Ce₂O₂S was determined for temperatures between 873 and 1073 K. This data was used to derive an empirical equation for ΔG_f° of Ce₂O₂S in this temperature range. This equation along with thermodynamic data for cerium oxides and sulfides obtained from the literature was used to predict Ce-O-S phase diagrams at 873 and 973 K. These phase diagrams provide insight into the mechanism of the deactivation of ceria-based catalysts by sulfur under reducing conditions.

Introduction

Understanding the interaction of sulfur with ceria is important in a variety of applications where ceria is used as a catalyst, catalyst support, or sorbent [1-6]. These applications range from automotive emissions control to sulfur removal from fuels and flue gasses, to solid oxide fuel cells. For example, in the three-way automotive emissions control catalyst ceria is used to provide oxygen storage capacity, which increases the range of air-to-fuel ratios in which the catalyst can operate. Exposure of ceria to even small amounts of sulfur-containing compounds significantly decreases ceria's oxygen storage capacity [1, 7, 8] and the overall catalyst performance. This deleterious effect of sulfur on ceria is one of the prime driving forces for recently enacted government regulations in both the United States and Europe that mandate substantial reduction in fuel sulfur content.

We have recently shown that ceria is an excellent hydrocarbon oxidation catalyst for use in the anode of a solid oxide fuel cell. Composite anodes composed of mixtures of Cu, CeO₂, and yttria-stabilized zirconia (YSZ) have been shown to be active for the direct electrochemical oxidation of hydrocarbons and highly resistant to fouling via carbon deposition [9-12]. This is in contrast to the more commonly used Ni/YSZ cermet anodes that rapidly deactivate due to coke deposition when exposed to dry hydrocarbons. As is the case for automotive catalysts, ceria-based SOFC anode catalysts are also affected by sulfur impurities in the fuel. This is illustrated by the data of Kim et al. [13] in Figure 1 which displays the current output at 0.5 V for a SOFC with a Cu/Ceria anode while operating on a fuel gas composed of 50 mol % decane in N₂ before and after the addition of 5000 ppm of S to the fuel. While operating on the decane/N₂ mixture the cell

exhibits stable operation. Introduction of 5000 ppm of sulfur, however, produces a 50 % decrease in the current output. It has been shown that this decrease is due to poisoning of the oxidation activity of the ceria.

Under oxidizing conditions, sulfur reacts with ceria to form cerium sulfates [4, 14]. In the case of automotive catalysts it is commonly thought that sulfate formation reduces the ability of the ceria to manage the oxygen partial pressure in the catalytic converter [1]. It is important to note, however, that while sulfates undoubtedly play a role in the deactivation of ceria under oxidizing conditions, different sulfur containing compounds may be formed under reducing conditions [5, 6, 15-17]. A detailed knowledge of cerium-sulfur chemistry under reducing conditions is therefore needed in order to fully understand sulfur deactivation of ceria. This is especially true in the applications mentioned above. During operation an automotive catalytic converter rapidly oscillates between oxidizing and reducing conditions. The gas exposed to the anode in a SOFC is also highly reducing.

In order to provide a more detailed understating of sulfur deactivation of ceria, especially under reducing conditions, we have recently used TPD, FTIR, and XPS to study the reaction of sulfur with ceria [15, 16]. These and other studies [1, 18, 19] show that SO₂ poisoning of ceria involves the formation of a complex set of compounds. As expected, under oxidizing conditions SO₂ reacts with ceria to form sulfates and sulfites. In contrast, under reducing conditions oxysulfides are formed. The inter-conversion between these various species upon changing the gas environment also appears to be rather facile. This complexity can be understood by considering a Ce-O-S phase diagram. Figure 2 displays the Ce-O-S phase diagram at 1100 K reported by Kay et al.

[20]. This phase diagram is based, for the most part, on free energies of formation that were measured at temperatures above 1100 K [20-23]. The phase diagram shows that for $P_{O_2} > 0.1$ atm, $Ce_2(SO_4)_3$ is the only stable sulfur containing species. Under more reducing conditions, the situation is much more complex and depending on the P_{S_2} cerium oxysulfide (Ce_2O_2S) and various cerium sulfides (CeS , Ce_3S_4 , and Ce_2S_3) can be formed.

From the perspective of using ceria-based catalysts under reducing conditions, the most important part of the phase diagram displayed in Figure 2 is the boundary between the cerium oxides and the cerium oxysulfide. This boundary in effect defines the P_{S_2} at which sulfur poisoning of ceria would be expected to occur. The temperature of this phase diagram, 1100 K, is at the upper end of the range that is of interest for most applications that make use of ceria catalysts. Thus, it is important to examine the Ce-O-S phase diagram at lower temperatures.

Kay et al. have compiled the necessary free energy and heat capacity data to allow one to calculate the Ce-O-S phase diagram at lower temperatures [20]. This data is listed in Table 1. Note that the most uncertain values in the table are those for Ce_2O_2S . The values for ΔH_f° , S° and C_p for this compound have not been measured directly. The values reported in the table for S° and C_p are a weighted average of those for Ce_2O_3 and Ce_2S_3 [20] and the value for ΔH_f° of Ce_2O_2S was chosen to be consistent with that measured by Dwiendi and Kay at 1072 K [21]. In light of this, the uncertainty in the phase boundary between Ce_2O_2S and CeO_x is quite large when this data is used to predict phase diagrams at temperatures below 1072 K. This is unfortunate since this phase boundary is critical in predicting the effect of sulfur on the performance of ceria-based

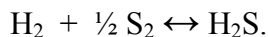
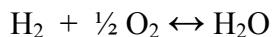
catalysts under reducing conditions. The motivation for the work described in this paper was, therefore, to examine the phase boundary between cerium oxides and cerium oxysulfide as a function of temperature for O_2 and S_2 partial pressures in ranges of interest for applications using ceria-based catalysts.

Experimental Methodology

Phase diagrams based on the data reported by Kay et al. [20] were used as a guide to estimate P_{S_2} and P_{O_2} values which correspond to conditions near the cerium oxide-cerium oxysulfide phase boundary for temperatures between 873 and 1073 K. The formation, or lack thereof, of the oxysulfide for these conditions was then determined. This was done by annealing a CeO_2 sample in a flowing gas stream with known values of P_{S_2} and P_{O_2} at the desired temperature. After equilibrium between the solid and gas phases had been established, temperature programmed oxidation (TPO) was used to determine if bulk Ce_2O_2S had been formed.

The experiments were carried out using a small flow reactor, which was contained in a tube furnace. The reactor was attached to a gas handling system that was equipped with mass flow controllers and allowed for the mixing of up to four individual gas streams. The specific gasses connected to the system in this study were He, O_2 , H_2 , and 1030 ppm H_2S in He. Water was introduced into the gas stream by flowing He through a bubbler containing H_2O . During an experiment, the gas handling system was used to flow a gas with known partial pressures of He, H_2 , H_2O and H_2S through the reactor containing the ceria sample. The partial pressures of O_2 and S_2 in the reactor were

determined by assuming that the following reactions were in equilibrium inside the reactor:



The thermodynamics of the formation of $\text{Ce}_2\text{O}_2\text{S}$ was studied for temperatures of 873, 973 and 1073 K.

In a typical experiment the CeO_2 sample was initially pre-treated by heating to 973 K in a flowing stream of 10 mole % O_2 in He and then annealed for five minutes at this temperature in 10 mole % H_2 in He. The sample was then exposed to a flowing stream of He, O_2 , H_2 , and H_2S and held at the desired temperature until equilibrium had been established. **Based on a study of the of the composition of the sample as a function of annealing time for conditions in which $\text{Ce}_2\text{O}_2\text{S}$ was formed, it was determined that an annealing time of one hour was sufficient in order to obtain the equilibrium composition.** After annealing sample was then rapidly quenched to approximately 620 K in flowing He.

After quenching, TPO was used to determine the composition of the sample. During a TPO run the sample was heated to 1173 K with a linear temperature ramp of 20 K/min in a flowing stream of 10 mole % O_2 in He. A small portion of the effluent from the reactor was admitted into a vacuum system containing a mass spectrometer, which was used to identify reaction products. For samples that contained sulfur, SO_2 was produced in a sharp peak centered at 1100 K. An example of this is shown in curve A in Figure 3, which was obtained from a ceria sample that had been exposed to 10^{-7} and $10^{-20.4}$ atm of S_2 and O_2 , respectively at 1073 K. Curve B in this figure corresponds to

SO₂ desorption from a ceria sample that was exposed to 10⁻⁸ and 10^{-20.6} atm of S₂ and O₂, respectively at 1073 K. Note that this latter treatment did not result in the production of the oxysulfide and the SO₂ desorption curve is flat.

The available thermodynamic data indicate that for the conditions used in this study the only sulfur-containing compound that should be formed is Ce₂O₂S. It is possible, however, that the thermodynamics of the formation of surface sulfide species may be different than that for bulk Ce₂O₂S. Quantification of the TPO SO₂ desorption peak was, therefore, used to determine if bulk Ce₂O₂S was indeed formed. This required a calibration factor for the SO₂ peak area. This calibration factor was measured by performing a TPO experiment with a known amount of Ce(SO₄)₂ using the same flow rate of the O₂/He mixture that was used in the TPO experiments with O₂/S₂-exposed ceria samples. During TPO with the Ce(SO₄)₂ sample, SO₂ was also produced at 1100 K. The calibration factor for the SO₂ peak was determined by dividing the area of this peak by the number of moles of sulfur in the Ce(SO₄)₂ sample. Based on quantification of the amount of SO₂ produced during TPO it was determined that the molar Ce:S ratio in all of the O₂/S₂-treated ceria samples that exhibited SO₂ peaks during TPO was approximately 2:1 which is consistent with the formation of bulk Ce₂O₂S.

Results and Discussion

Figure 4 displays a portion of the Ce-O-S phase diagram for P_{O₂} between 10⁻⁴⁰ and 10⁻²⁰ atm and P_{S₂} between 10⁻³⁰ and 1 atm at 1073 K which is based on the data in Table 1. Since Kay et al. [20, 21] measured ΔG_f for Ce₂O₂S at 1073 K, the phase boundary between Ce₂O₂S and the various cerium oxides at this temperature should be

fairly accurate. Note that in addition to CeO_2 and Ce_2O_3 the phase diagram contains $\text{CeO}_{1.72}$ and $\text{CeO}_{1.83}$. As discussed in a recent review by Mogensen et al. [24] there is some data in the literature that indicates that other cerium sub-oxide phases may exist in this region of the phase diagram. Unfortunately, the stoichiometries of these other phases have yet to be unambiguously determined. Since the free energies of formation and the heat capacities of these additional phases should fall between those for CeO_2 and Ce_2O_3 , as do those for $\text{CeO}_{1.72}$ and $\text{CeO}_{1.83}$, the inclusion of these additional phases would have little effect on the location of the phase boundary between $\text{Ce}_2\text{O}_2\text{S}$ and CeO_x .

The data points in the figure were measured in the present study using the procedure described above. The circles and triangles correspond to conditions for which the TPO results showed the formation of $\text{Ce}_2\text{O}_2\text{S}$, and cerium oxide, respectively. Note that the data points collected in this study are consistent with the phase boundary between $\text{Ce}_2\text{O}_2\text{S}$ and $\text{CeO}_{1.83}$ predicted by the thermodynamic data reported by Kay et al. [20]. This is an important result and provides a verification of the experimental methodology used in the present study.

Figures 5 and 6 display Ce-O-S phase diagrams based on the thermodynamic data in Table 1 for reducing conditions and temperatures of 973 and 873 K. The individual data points in the figures were measured in the present study with the circles and triangles again corresponding to conditions for which the TPO showed the formation of $\text{Ce}_2\text{O}_2\text{S}$, and cerium oxides, respectively. The equilibrium phase boundary between $\text{Ce}_2\text{O}_2\text{S}$ and $\text{CeO}_{1.83}$ can be estimated based on the experimental data points. The data shows that the phase boundary at 973 K occurs at S_2 partial pressures that are approximately one order of magnitude higher than those predicated by the thermodynamic data in Table 1. As

shown in Figure 6, at 873 K this phase boundary occurs at S₂ partial pressures that are approximately three orders of magnitude higher than those predicated by the thermodynamic data in Table 1.

Fitting values of ΔG_f for Ce₂O₂S that were determined using the estimated values for ΔH_f° , S° and C_p reported by Kay et al. [20] in Table 1 to a function of temperature results in the following equation:

$$\Delta G_f = -0.32 T - 1574.5 \quad \text{for} \quad 673 \text{ K} < T < 1073 \text{ K} \quad (1)$$

(ΔG_f [=] kJ/mol, T [=] K, reference states: pure components at 298 K and 1 atm)

As noted above, the data in Figures 5 and 6 show that this equation over estimates the magnitude of the free energy of formation for the oxysulfide. The phase boundary between Ce₂O₂S and CeO_{1.83} determined experimentally can be used to provide a more accurate estimate of ΔG_f for Ce₂O₂S as a function of temperature. Fitting of this data gives rise to the following equation for ΔG_f :

$$\Delta G_f = -0.43 T - 1456.9 \quad \text{for} \quad 873 \text{ K} < T < 1073 \text{ K} \quad (2)$$

(ΔG_f [=] kJ/mol, T [=] K, reference states: pure components at 298 K and 1 atm)

The dotted lines in Figures 5 and 6 correspond to the phase boundaries between Ce₂O₂S, Ce₂S₃ and the various cerium oxides that were calculated using values of ΔG_f of Ce₂O₂S from equation 2. At least over this limited temperature range, these phase boundaries should be more accurate than those predicted using the data of Kay et al. [20].

The calculated Ce-O-S phase diagrams displayed in Figures 4 through 6 provide a useful starting point for understanding the effect of sulfur on ceria-based catalysts under reducing conditions. For example, they provide insight into the fuel cell performance data presented in Figure 1. In this example the power output of the fuel cell at 973 K while operating on a fuel composed of 50 mole % n-decane in N₂ decreased by approximately 50 % upon the addition of 5000 ppm of sulfur. Based on the overall fuel conversion and assuming equilibrium in the gas phase, the partial pressures of O₂ and S₂ in the cell were estimated to be 10^{-25.5} and 10^{-12.6} atm, respectively [13]. These conditions correspond to the diamond displayed in Figure 5. Note that this datum point falls within the Ce₂O₂S region of the phase diagram. This indicates that the decrease in performance upon the introduction of 5000 ppm sulfur was due to the formation of the oxysulfide.

The phase diagram also suggests that the ceria catalyst should not be seriously affected at more modest sulfur levels in the fuel. Indeed this has been experimentally verified and an identical fuel cell showed no performance degradation when 100 ppm of sulfur was added to a 5 mole % n-decane in N₂ fuel while operating at 973 K [13]. The calculated P_{O₂} and P_{S₂} in this case were 10^{-26.6} and 10^{-20.3} atm, respectively which correspond to the square in Figure 5. Note that this datum point falls in the CeO_{1.72} region of the phase diagram.

These phase diagrams also have implications for the use of ceria in automotive exhaust catalysts. As noted above, the poisoning of ceria's oxygen storage capacity by sulfur is generally attributed to the formation of cerium sulfates [1, 7, 8]. Although this may be the case under oxidizing conditions, under reducing conditions other sulfur containing species such as the oxysulfide may be formed. Partial pressures of O₂ that are

low enough to result in oxysulfide formation are not likely to occur at the inlet to a catalytic converter even during fuel rich excursions. The P_{O_2} will obviously decrease significantly, however, down the length of the converter. Equilibrium calculations can be used to estimate a lower bound on the P_{O_2} that would be present in a catalytic converter under typical operating conditions during a fuel rich excursion. This type of calculation indicates that a P_{O_2} as low as 10^{-30} atm is not unreasonable. Thus, the results of this study suggest that the formation of oxysulfides must be considered when assessing the effects of sulfur on the performance of three-way automotive catalysts.

Conclusions

In this study the phase boundary between Ce_2O_2S and $CeO_{1.83}$ was measured for temperatures between 873 and 1073 K. The location of this phase boundary was used to derive an empirical equation for ΔG_f of Ce_2O_2S as a function of temperature. This equation along with thermodynamic data from the literature was used to calculate the equilibrium phase boundaries between the various cerium oxides, Ce_2O_2S , and Ce_2S_3 . The calculated phase diagrams show that at temperatures between 673 and 1073 K, the formation of Ce_2O_2S requires significantly higher sulfur partial pressures than those suggested in previous studies. The Ce-O-S phase diagrams reported in this study provide a useful starting point for understanding the effect of sulfur on the performance ceria-based catalysts under reducing conditions

Acknowledgements

This work was supported by the DARPA Palm Power Program.

References

1. M. Boaro, C. de Leitenburg, G. Dolcetti, A. Trovarelli, M. Graziani, Topics in Catalysis 16 (2001) 299.
2. M. Flytzani-Stephanopoulos, Mrs Bull 26 (2001) 885.
3. Y. Zeng, S. Zhang, F. R. Groves, D. P. Harrison, Chem Eng Sci 54 (1999) 3007.
4. R. J. Gorte, T. Luo, Catalytic Science Series 2 (2002) 377.
5. M. Kobayashi, M. Flytzani-Stephanopoulos, Ind. Eng. Chem. Res. 41 (2002) 3115.
6. Z. Li, M. Flytzani-Stephanopoulos, Ind. Eng. Chem. Res. 36 (1997) 187.
7. D. D. Beck, J. W. Sommers, C. L. DiMaggio, Appl. Catal. B-Environ. 11 (1997) 273.
8. D. D. Beck, J. W. Sommers, C. L. Dimaggio, Appl. Catal. B-Environ. 3 (1994) 205.
9. R. J. Gorte, H. Kim, J. M. Vohs, J Power Sources 106 (2002) 10.
10. S. Park, R. J. Gorte, J. M. Vohs, Appl. Catal. A-Gen. 200 (2000) 55.
11. S. D. Park, J. M. Vohs, R. J. Gorte, Nature 404 (2000) 265.
12. H. Kim, S. Park, J. M. Vohs, R. J. Gorte, J. Electrochem. Soc. 148 (2001) A693.
13. H. Kim, J. M. Vohs, R. J. Gorte, Chem. Commun. 2001) 2334.
14. M. Waqif, P. Bazin, O. Saur, J. C. Lavalley, G. Blanchard, O. Touret, Appl. Catal. B-Environ. 11 (1997) 193.
15. T. Luo, J. M. Vohs, R. J. Gorte, J. Catal. 210 (2002) 397.
16. R. M. Ferrizz, R. J. Gorte, J. M. Vohs, Catal. Lett. in press (2002).
17. Y. Zeng, S. Kaytakoglu, D. P. Harrison, Che. Eng. Sci. 55 (2000) 4893.
18. J. A. Rodriguez, T. Jirsak, A. Freitag, J. C. Hanson, J. Z. Larese, S. Chaturvedi, Catal. Lett. 62 (1999) 113.

19. S. H. Overbury, D. R. Mullins, D. R. Huntley, L. Kundakovic, *J. Phys. Chem. B* 103 (1999) 11308.
20. D. A. R. Kay, W. G. Wilson, V. Jalan, *J Alloy Compd* 193 (1993) 11.
21. R. K. Dwivedi, D. A. R. Kay, *J Less-Common Met* 102 (1984) 1.
22. I. Barin, O. Knacke, *Thermochemical Properties of Inorganic Substances*, Springer-Verlag, New York, 1973, .
23. I. Barin, O. Knacke, *Thermochemical Properties of Substances - Supplement*, Springer-Verlag, New York, 1977, .
24. M. Mogensen, N. M. Sammes, G. A. Tompsett, *Solid State Ionics* 129 (2000) 63.

Figure Captions

Figure 1. Performance of a SOFC as a function of time at 973 K while holding the cell potential at 0.5 V [8]. During the first two hours the feed to the anode was 50 mole % n-decane in N₂ and then 5000 ppm of sulfur was added to the fuel.

Figure 2. Ce-O-S phase diagram at 1100 K based on the data in Table 1.

Figure 3. Sulfur dioxide desorption curves during TPO from samples that were previously treated in (A) 10⁻⁷ and 10^{-20.4} atm of S₂ and O₂, respectively at 1073 K and (B) 10⁻⁸ and 10^{-20.6} atm of S₂ and O₂, respectively at 1073 K.

Figure 4. Ce-O-S phase diagram at 1073 K based on the data in Table 1. The data points in the figure were measured in the present study. The circles and triangles correspond to conditions for which Ce₂O₂S, and cerium oxide are stable, respectively.

Figure 5. Ce-O-S phase diagram at 973 K based on the data in Table 1. The data points in the figure were measured in the present study. The circles and triangles correspond to conditions for which Ce₂O₂S, and cerium oxide are stable, respectively. The dotted lines are based on the ΔG_f of Ce₂O₂S measured in the present study.

Figure 6. Ce-O-S phase diagram at 873 K based on the data in Table 1. The data points in the figure were measured in the present study. The circles and triangles correspond to conditions for which $\text{Ce}_2\text{O}_2\text{S}$, and cerium oxide are stable, respectively. The square and diamond data points were obtained in a study of the effect of sulfur on the performance of a SOFC and are described in the text. The dotted lines are based on the ΔG_f of $\text{Ce}_2\text{O}_2\text{S}$ measured in the present study.